Changes in the North Atlantic Oscillation influence CO_2 uptake in the North Atlantic over the past 2 decades

Helmuth Thomas,[1] A. E. Friederike Prowe,[1,2] Ivan D. Lima,[3] Scott C. Doney,[3] Rik Wanninkhof,[4] Richard J. Greatbatch,[1,5] Ute Schuster,[6] and Antoine Corbière[7]

Received 12 December 2007; revised 1 August 2008; accepted 11 August 2008; published 31 December 2008.

[1] Observational studies report a rapid decline of ocean CO_2 uptake in the temperate North Atlantic during the last decade. We analyze these findings using ocean physical-biological numerical simulations forced with interannually varying atmospheric conditions for the period 1979–2004. In the simulations, surface ocean water mass properties and CO_2 system variables exhibit substantial multiannual variability on sub-basin scales in response to wind-driven reorganization in ocean circulation and surface warming/cooling. The simulated temporal evolution of the ocean CO_2 system is broadly consistent with reported observational trends and is influenced substantially by the phase of the North Atlantic Oscillation (NAO). Many of the observational estimates cover a period after 1995 of mostly negative or weakly positive NAO conditions, which are characterized in the simulations by reduced North Atlantic Current transport of subtropical waters into the eastern basin and by a decline in CO_2 uptake. We suggest therefore that air-sea CO_2 uptake may rebound in the eastern temperate North Atlantic during future periods of more positive NAO, similar to the patterns found in our model for the sustained positive NAO period in the early 1990s. Thus, our analysis indicates that the recent rapid shifts in CO_2 flux reflect decadal perturbations superimposed on more gradual secular trends. The simulations highlight the need for long-term ocean carbon observations and modeling to fully resolve multiannual variability, which can obscure detection of the long-term changes associated with anthropogenic CO_2 uptake and climate change.

Citation: Thomas, H., A. E. Friederike Prowe, I. D. Lima, S. C. Doney, R. Wanninkhof, R. J. Greatbatch, U. Schuster, and A. Corbière (2008), Changes in the North Atlantic Oscillation influence CO_2 uptake in the North Atlantic over the past 2 decades, *Global Biogeochem. Cycles*, *22*, GB4027, doi:10.1029/2007GB003167.

1. Introduction

[2] During the last decade, increasing observational efforts have been undertaken to gain insight into the variability of the North Atlantic Ocean CO_2 sink, which plays a crucial role in marine and global carbon cycles by transferring CO_2 from the atmosphere into the ocean [e.g., *Takahashi et al.*, 1997]. Several recent studies, covering the Gulf Stream/North Atlantic Current regions including polar extensions [*Lefèvre et al.*, 2004; *Omar and Olsen*, 2006; *Olsen et al.*, 2006; *Lüger et al.*, 2006; *Corbière et al.*, 2007; *Schuster and Watson*, 2007], report a more rapid rise of surface ocean pCO_2 than of atmospheric pCO_2 during the last decade (Figure 1). Accordingly, the sea-air CO_2 partial pressure difference (ΔpCO_2, i.e., surface ocean pCO_2 minus atmospheric pCO_2) shifts in a positive direction, that is toward a smaller sink or larger source, and the net ocean CO_2 uptake declines. In contrast, sea-air ΔpCO_2 remained approximately constant in some North Atlantic regions, such as at the Bermuda Times Series station (BATS) [*Bates*, 2001, 2007], or exhibited negative trends somewhat north of BATS [*Lüger et al.*, 2006] (Figure 1). Although there has been no conclusive attribution for these findings, possible explanations include rising temperatures [*Corbière et al.*, 2007], declining rates of subsurface water ventilation [*Schuster and Watson*, 2007], changes in biological activity [*Lefèvre et al.*, 2004], and the uptake of anthropogenic CO_2 itself, which can increase the sea-air ΔpCO_2 either locally

[1]Department of Oceanography, Dalhousie University, Halifax, Nova Scotia, Canada.
[2]Marine Biogeochemistry Research Division, Leibniz-Institut für Meereswissenschaften, IFM-GEOMAR, Kiel, Germany.
[3]Department of Marine Chemistry and Geochemistry, Woods Hole Oceanographic Institution, Woods Hole, Massachusetts, USA.
[4]Ocean Chemistry Division, Atlantic Oceanographic and Meteorological Laboratory, NOAA, Miami, Florida, USA.
[5]Theoretical Oceanography Department, Leibniz-Institut für Meereswissenschaften, IFM-GEOMAR, Kiel, Germany.
[6]School of Environmental Sciences, University of East Anglia, Norwich, UK.
[7]Laboratoire d'Océanographie et du Climat: Expérimentation et Approches Numériques, IPSL, Université Pierre et Marie Curie, Paris, France.

0886-6236/08/2007GB003167$12.00

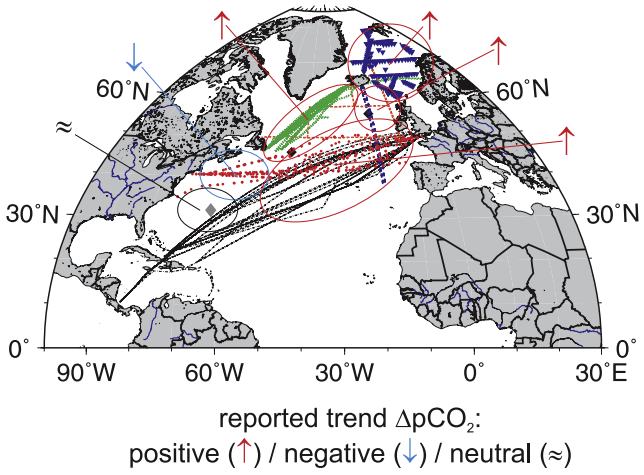

Figure 1. Locations and general trends of recent surface ocean CO_2 studies in the North Atlantic. The gray diamond indicates Bermuda Times Series station (BATS) [*Bates*, 2001, 2007]; red boxes [*Lefèvre et al.*, 2004] and red [*Lüger et al.*, 2006], blue [*Omar and Olsen*, 2006; *Olsen et al.*, 2006], green [*Corbière et al.*, 2007], and black [*Schuster and Watson*, 2007] tracks indicate locations of recent observational field studies. Most of the field studies cover the period 1995 until 2002/2004. The main sea-air ΔpCO_2 trends, as obtained by the field studies, have been indicated. Red upward pointing arrows indicate positive ΔpCO_2 trends; the blue downward pointing arrow signifies a negative trend, and the symbol "≈" indicates no change in ΔpCO_2. The black diamonds indicate the locations at 56.1°N/18.5°W and 45.8°N/43.6°W (see Figures 7–9).

or as an advected signal [*Omar and Olsen*, 2006; *Olsen et al.*, 2006; *Thomas et al.*, 2007]. The rates of change of ΔpCO_2 appear to accelerate in northward direction and this might be related to the northward decrease in seawater CO_2 buffer capacity [*Olsen et al.*, 2006; *Thomas et al.*, 2007; *Sabine et al.*, 2004].

[3] The temperature, freshwater balance, and circulation of the North Atlantic Ocean have undergone substantial alterations during recent decades due to anthropogenic climate change and natural climate variability, resulting in overall warmer, more saline surface waters in lower latitudes and fresher surface waters in higher latitudes [e.g., *Fung et al.*, 2005; *IPCC*, 2001; *Curry et al.*, 2003; *Curry and Mauritzen*, 2005]. Many of the changes in ocean climate and circulation are in response to variations in the North Atlantic Oscillation (NAO), the dominant atmospheric climate mode in the basin on interannual to decadal timescales. During positive phases of the NAO, surface pressure decreases in the Icelandic low and increases in the Azores high, leading to stronger surface westerly winds, a northward shift of storm tracks, and altered cooling, evaporation and precipitation patterns.

[4] Here we analyze the mechanisms governing surface water pCO_2 variability in the context of NAO driven variability using an ocean model hindcast simulation [*Lovenduski et al.*, 2007; *Doney et al.*, 2007, 2008a], which broadly reproduces the observed North Atlantic trends of sea-air ΔpCO_2 during the last decade. Our results suggest that a component of the positive sea-air ΔpCO_2 trend over the last decade occurred as the result of a shift from largely positive NAO index prior to 1995 to a period of mostly weakly positive or negative NAO. The rapid temporal shift in ΔpCO_2 appears, in fact, to be anomalous with respect to the longer-term secular trends, which are significantly less pronounced. Moreover, our simulations exhibit intermittent periods of opposing trends (more negative ΔpCO_2) in certain regions and time periods. After introducing our methods, we discuss relevant hydrodynamic responses of the North Atlantic Ocean to changes in the NAO index. Then we relate these findings to the variability of the CO_2 system before closing with a synthesis of our results in the light of recent observations.

2. Methods

[5] Historical simulations using a global ocean carbon model are used to estimate the long-term trends of CO_2 air-sea fluxes and related parameters over the North Atlantic on a monthly resolution. The ocean model includes the biogeochemical cycling of C, O, N, P, Fe, Si, and alkalinity and four phytoplankton functional groups (diazotrophs, diatoms, pico/nano-plankton, and coccolithophores). The ecosystem module [*Moore et al.*, 2004] coupled to a modified version of the OCMIP-2 biogeochemistry code [*Doney et al.*, 2006; *Najjar et al.*, 2007] is embedded in the coarse-resolution Parallel Ocean Program (POP) ocean component of the Community Climate System Model (CCSM) [*Yeager et al.*, 2006]. The hindcast (1979–2004) is forced with interannually varying atmospheric physical and CO_2 data [*Doney et al.*, 2007, 1998a]. Model validations for selected parameters have been given by *Doney et al.* [2007, 2008a, 2008b]. We compare our simulations with CO_2 system observations [*Lüger et al.*, 2006; *Corbière et al.*, 2007; *Schuster and Watson*, 2007] for selected regions. For our mechanistic analysis we also refer to a model run with constant atmospheric CO_2 conditions (preindustrial run) in order to unravel physical climate driven variability from trends due to rising atmospheric CO_2 conditions.

[6] We employ salinity normalized alkalinity ($A_{T,norm}$) and dissolved inorganic carbon (DIC_{norm}) concentrations as water mass tracers using a mean salinity of 35; that is $DIC_{norm} = DIC*35/Sal_{in\ situ}$ and $A_{T,norm} = A_T*35/Sal_{in\ situ}$. The current model setup includes riverine freshwater inputs with zero salinity and with zero concentrations of DIC and A_T; river inputs, therefore, are equivalent to net precipitation minus evaporation. Thus, the application of the simple salinity normalization procedure, as compared to more sophisticated analyses such as the one proposed by *Friis et al.* [2003], introduces only minor error into our analysis.

[7] A regression analysis is used to unravel the mechanisms driving the simulated long-term trends of surface water pCO_2 and sea-air ΔpCO_2. Spatial trend maps are computed for each model property X from the local slope of the linear regression against time (δX). Regressions are calculated for the full hindcast (1979–2004) and for selected

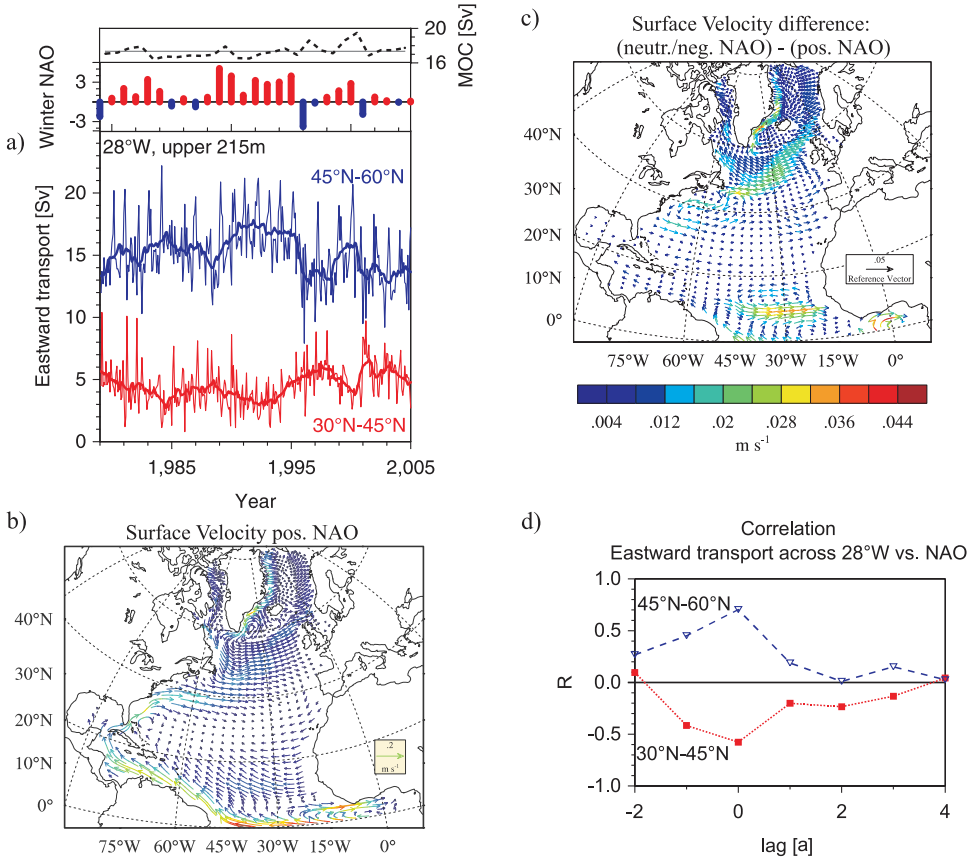

Figure 2. Hydrodynamic responses of the North Atlantic Ocean to North Atlantic Oscillation (NAO) forcing. (a) (top) Annual averages of Meridional Overturning Circulation (MOC) from 1979 to 2005. The thin line gives the mean MOC for the 1979–2004 period. (middle) Winter NAO index for the years 1979 to 2005. (bottom) Eastward transport of the upper 215 m of the water column for two sections along 28°W: from 60°N to 45°N (blue) and from 45°N to 30°N (red). The bold lines give the 12-month moving averages. (b) Surface velocities have been averaged for a positive NAO period (1989–1995). (c) Differences in mean surface velocities between a neutral/negative NAO period (1996–2004) and a positive NAO period (1989–1995) (neutral/negative NAO–positive NAO). (d) Correlation coefficient of annual mean eastward transport across 28°W for each of the above sections and the winter NAO are plotted against the lag time. The correlation coefficients have been established for a series of time lags (−2 to +4 years) between these parameters.

subperiods, including the 1995–2004 period, which covers the time when observational estimates show rapidly evolving ΔpCO_2. The δpCO_2 trends are decomposed using a linear Taylor expansion [*Lovenduski et al.*, 2007; *Doney et al.*, 2008a] into its governing processes: changes in salinity (S), temperature (T), salinity normalized DIC (DIC_{norm}) and salinity normalized alkalinity ($A_{T,norm}$):

$$\delta pCO_2 = \frac{\partial pCO_2}{\partial S_{FW}}\delta S + \frac{\partial pCO_2}{\partial T}\delta T + \frac{\partial pCO_2}{\partial DIC_{norm}}\delta DIC_{norm} + \frac{\partial pCO_2}{\partial A_{T,norm}}\delta A_{T,norm} \quad (1)$$

Precipitation and evaporation of freshwater and river inputs drive correlated variations in surface water DIC and A_T, which have opposing effects on pCO_2. To remove this effect, we use salinity normalized DIC_{norm} and $A_{T,norm}$, and the partial derivative with respect to salinity $\partial/\partial S_{FW}$ includes the effects of freshwater dilution on *DIC* and A_T.

3. Results

3.1. Responses of the North Atlantic Circulation to NAO Variability

[8] In this section, we briefly discuss the NAO driven variability of the circulation of the North Atlantic, particularly variations in surface velocity patterns. Under positive NAO conditions, such as during the 1989–1995 period, the North Atlantic Current (NAC), accelerates in the (north) eastward direction in response to the higher wind stresses (Figure 2). As a result more warm, saline subtropical water is transported toward the eastern subpolar gyre and polar

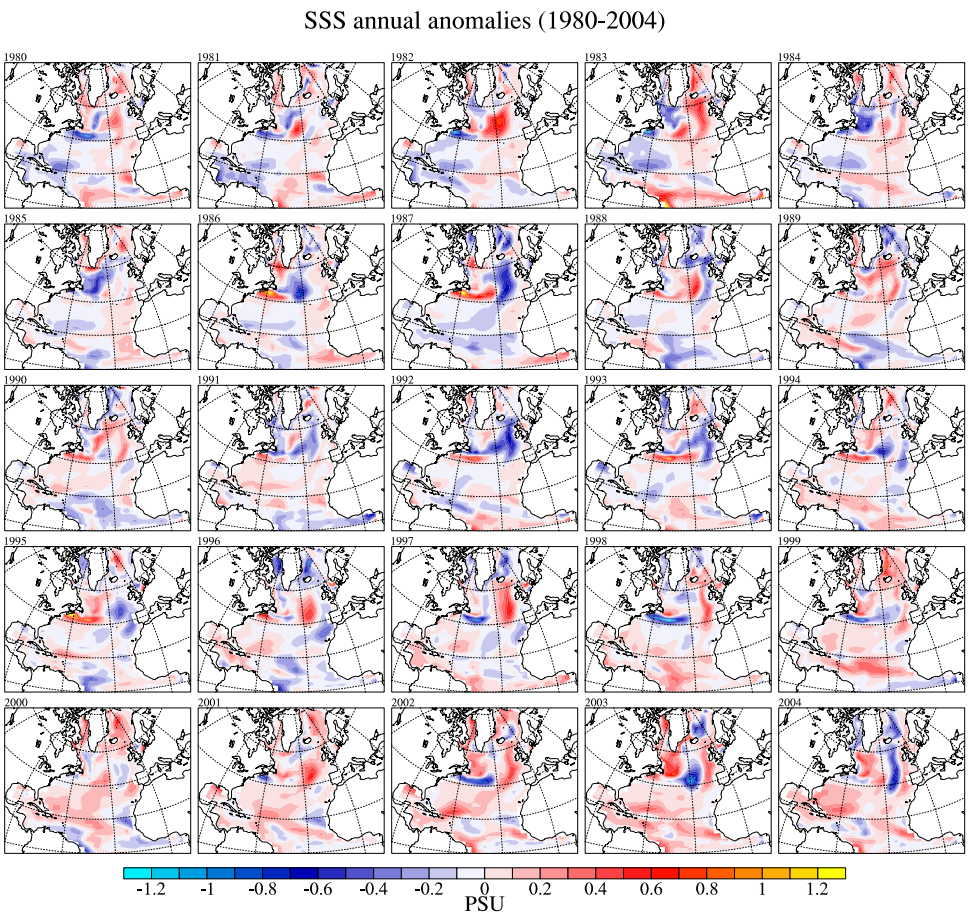

Figure 3. Annual averages of sea surface salinity (SSS) anomalies for the years 1980–2004.

seas. There is a corresponding reduction in transport into the return flow of the eastern subtropical gyre, as indicated by the temporal variations in integrated eastward transport across 28°W between 30–45°N. The transport in the eastern subtropical gyre is anticorrelated with the NAO with essentially zero lag. During positive NAO periods, the subtropical gyre also expands northward, evident from the buildup of a positive salinity anomaly at the boundary between the subpolar and subtropical gyre off the North American continent at approximately 45°N during the 1989–1995 period (Figure 3). The opposite circulation patterns occur during neutral or negative NAO conditions.

[9] The southward velocity of the Labrador Current and the eastward velocity of the southern limb of the subpolar gyre both also increase during positive NAO periods, bringing more fresh and cold waters of Arctic origin into the subpolar gyre (Figures 2b and 2c). Eastward transport is positively correlated with NAO, again with zero lag, across the northern (45–60°N) end of the 28°W section. Under neutral or negative NAO conditions, the NAC and the Labrador Current velocities weaken (Figure 2c), permitting Labrador Current Waters to spread along the eastern coast of North America (Figure 3, e.g., years 1996–2000). Our simulations are consistent in these respects with observational studies [e.g., *Flatau et al.*, 2003].

[10] Positive NAO phases enhance the deep convection in the Labrador Sea and thus lead to an enhancement of the Meridional Overturning Circulation (MOC) with a 5 to 10 year time lag after the onset of a positive NAO [*Eden and Jung*, 2001; *Eden and Greatbatch*, 2003] (Figure 2a). Moreover, it has been reported that the strong westerly winds during positive NAO phases cause an anticyclonic anomaly (i.e., a slowing down) of the subpolar gyre [*Greatbatch*, 2000; *Eden and Jung*, 2001; *Eden and Willebrand*, 2001; *Eden and Greatbatch*, 2003]. Both processes tend to partially counteract the NAO related surface circulation patterns reported above, but their effect is significantly weaker than the more dominant and immediate wind-driven reorganizations.

3.2. Simulated ΔpCO_2 Variability and Temporal Trends in the North Atlantic

[11] The CCSM simulations exhibit substantial anomalies in annual mean, deseasonalized sea-air ΔpCO_2 (+/−20 ppm) in response to varying atmospheric forcing and ocean circulation (Figure 4). The ΔpCO_2 anomalies have spatial scales of a few hundred to a few thousand km and often persist over multiannual timescales. The anomalies are typically subgyre scale; that is, multiple positive and negative anomalies occur simultaneously within either the subtropical or subpolar gyre.

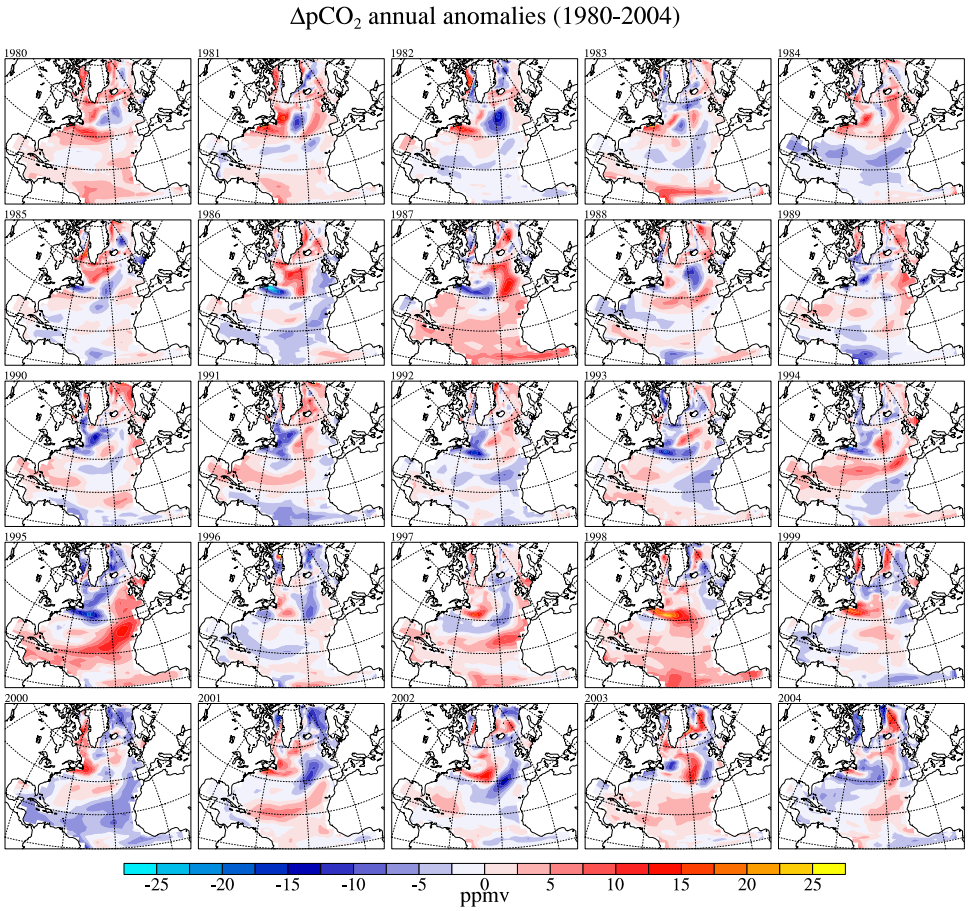

Figure 4. Annual averages of ΔpCO_2 anomalies for the years 1980–2004.

[12] Over the full simulation (1979–2004), model surface ocean pCO_2 rises gradually throughout the entire basin (Figure S1[1]), with areas that both slightly exceed or lag behind the atmospheric rate of approximately 1.6 ppm a^{-1}. This is illustrated in maps of the trend over time in sea-air ΔpCO_2 (Figure 5a). Positive trends for the sea-air ΔpCO_2 imply declining CO_2 uptake in undersaturated areas or increasing CO_2 release to the atmosphere in supersaturated areas. The broad similarity of the sea-air ΔpCO_2 trends between the anthropogenic CO_2 case (time-varying atmospheric CO_2) (Figure 5a) and the preindustrial CO_2 case (constant atmospheric CO_2) (Figure 5b) indicate that these patterns arise primarily because of ocean dynamics acting on surface water pCO_2 rather than the atmospheric CO_2 perturbations.

[13] Trend estimates for sea-air ΔpCO_2 are complicated on shorter, decadal timescales by regional interannual variability in surface water pCO_2. For example for the recent positive NAO period (1991–1996), the absolute magnitude of the simulated sea-air ΔpCO_2 trends (Figure 5c) are noticeably larger than the low-frequency (1979–2004) secular trends (Figure 5a). The 1991–1996 sea-air ΔpCO_2 trends are strongly positive in the subtropics and western subpolar gyre (surface water pCO_2 values growing faster than the atmospheric rate of 1.6 ppm a^{-1}) and strongly negative in the eastern subpolar gyre and polar seas. The subpolar sea-air ΔpCO_2 trends switch signs from the positive NAO period 1991–1996 to the neutral/negative NAO period 1997–2004 (Figure 5d).

3.3. Partitioning the Factors Driving ΔpCO_2 and pCO_2 Trends

[14] The NAO influences sea-air ΔpCO_2 by altering the surface water thermodynamic properties (S, T, DIC_{norm}, $A_{T,norm}$) governing seawater pCO_2 (equation (1)). These interactions occur via changes in air-sea heat and freshwater fluxes, biological fluxes, lateral transport, and vertical mixing. Visual inspection shows broad similarities in the annual sea-air ΔpCO_2 anomaly patterns (Figure 4) with comparable anomaly maps for salinity (Figure 3), DIC_{norm} (Figure S4), and temperature (Figure S5). For example, salinity and ΔpCO_2 anomalies are typically anticorrelated, particularly evident during years of Great Salinity Anomaly events such as during 1984–1987 or 1991–1993.

[15] A linear decomposition of pCO_2 variations following equation (1) leads to a more quantitative analysis of the factors governing pCO_2 temporal trends (see Figure S1). In

[1]Auxiliary materials are available in the HTML. doi:10.1029/2007GB003167.

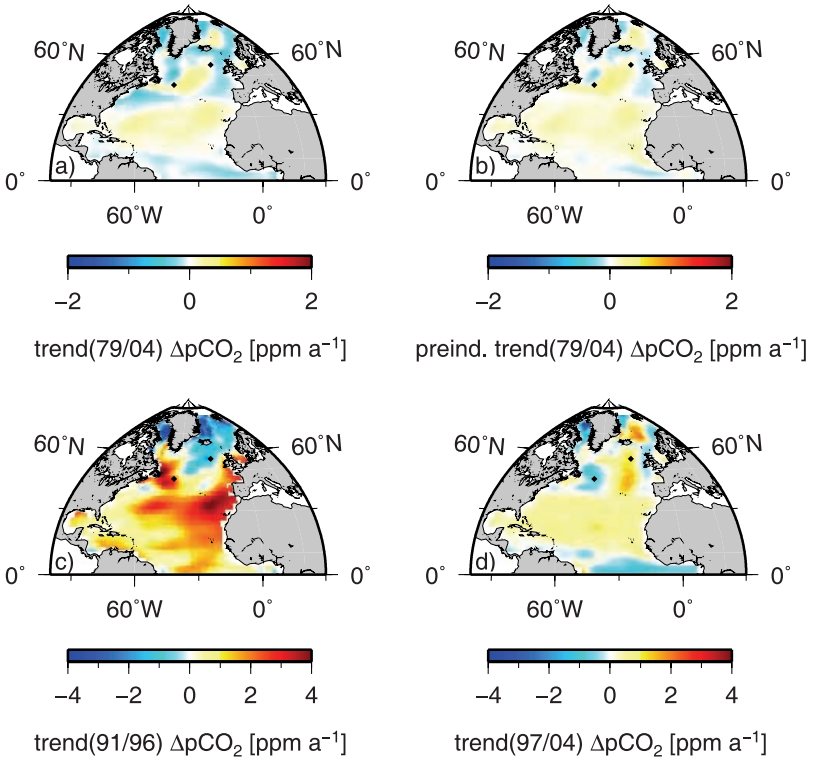

Figure 5. Trend regression analysis of sea-air ΔpCO_2 for selected periods. Regressions of simulated sea-air ΔpCO_2 for the periods 1979–2004 for the (a) anthropogenic and (b) preindustrial runs. The correlation coefficient between the trends of both runs for the 1979–2004 period is R = 0.93 with N = 1764 and a standard deviation of the residuals of 0.094. Regressions of simulated sea-air ΔpCO_2 for the periods (c) 1991–1996 and (d) 1997–2004 for the anthropogenic run, respectively. Please refer to Figures 7 and 8 for details regarding the choice of the 1991–1996 period. The black diamonds indicate the locations at 56.1°N/18.5°W and 45.8°N/43.6°W (see Figures 8 and 9). Please note the change of color scale in Figures 5c and 5d.

the anthropogenic CO_2 case (1979–2004), surface water pCO_2 trends are uniformly positive as expected because of anthropogenic CO_2 uptake and the resulting positive trends in surface water DIC_{norm} (Figure S1d). We remove this anthropogenic CO_2 trend and isolate the signals caused by ocean circulation variability using a companion preindustrial CO_2 simulation with constant atmospheric CO_2 conditions (but the same time-varying atmospheric physical forcing). The preindustrial case pCO_2 trends and the components due to S, T, DIC_{norm}, $A_{T,norm}$ trends are shown in Figure 6 for 1991–1996 and in Figure 7 for 1997–2004.

[16] The dominant factors driving simulated pCO_2 trends differ by region and time period, and the overall pCO_2 trend often reflects the net balance of larger, opposing forcing trends. For 1991–1996 (positive NAO), warming of the NAC and subpolar gyre (positive pCO_2 trend) is countered by a trend to more saline, lower-DIC_{norm} conditions (negative pCO_2 trend). The relative strengths of warming versus saline/lower DIC_{norm} differ from the western to eastern basin, resulting in a dipole pattern in overall pCO_2 trend. The effects of DIC_{norm} and $A_{T,norm}$ are largely anticorrelated, dominated in their sum $pCO_{2\ (DICnorm\ \&\ Alk,norm)}$ by the DIC_{norm} pattern. The thermodynamic forcing terms are more in phase in the subtropics, with warming, freshening, and elevated DIC_{norm} all contributing to positive pCO_2. As discussed above for ΔpCO_2 trends, the 1997–2004 (neutral/negative NAO) pCO_2 trends flip sign in the NAC and subpolar gyre because of a reversal of the regional trends in warming/cooling, salinity and DIC_{norm}. The longer-term secular trends (1979–2004) in pCO_2 due to T, S and $A_{T,norm}$ are substantially weaker or even vanish (Figure S1), which is the case for the ΔpCO_2 as well (Figure 4).

[17] To further illustrate the impact of climate variability on ΔpCO_2 trends, we examine time series of surface water at two locations in the eastern (56.1°N/18.5°W, Figure 8) and western (45.8°N/43.6°W, Figure 9) NAC/subpolar gyre. Both locations exhibit substantial multiannual variability in DIC_{norm}, salinity, temperature and sea-air ΔpCO_2. Consistent with the regional maps (Figures 6 and 7), periods of sharply increasing DIC_{norm} at each location tend to occur when surface salinity is declining and temperature is rising. The western and eastern sides of the subpolar gyre are out of phase, with large surface freshening and increasing DIC_{norm} in the west prior to 1995 and in the east after 1997.

[18] The dipole-like spatial behavior in model pCO_2 trends at these two locations can be attributed to variations of the NAO index, which was anomalously positive from 1989 to 1995 and then reverted mostly to more neutral or

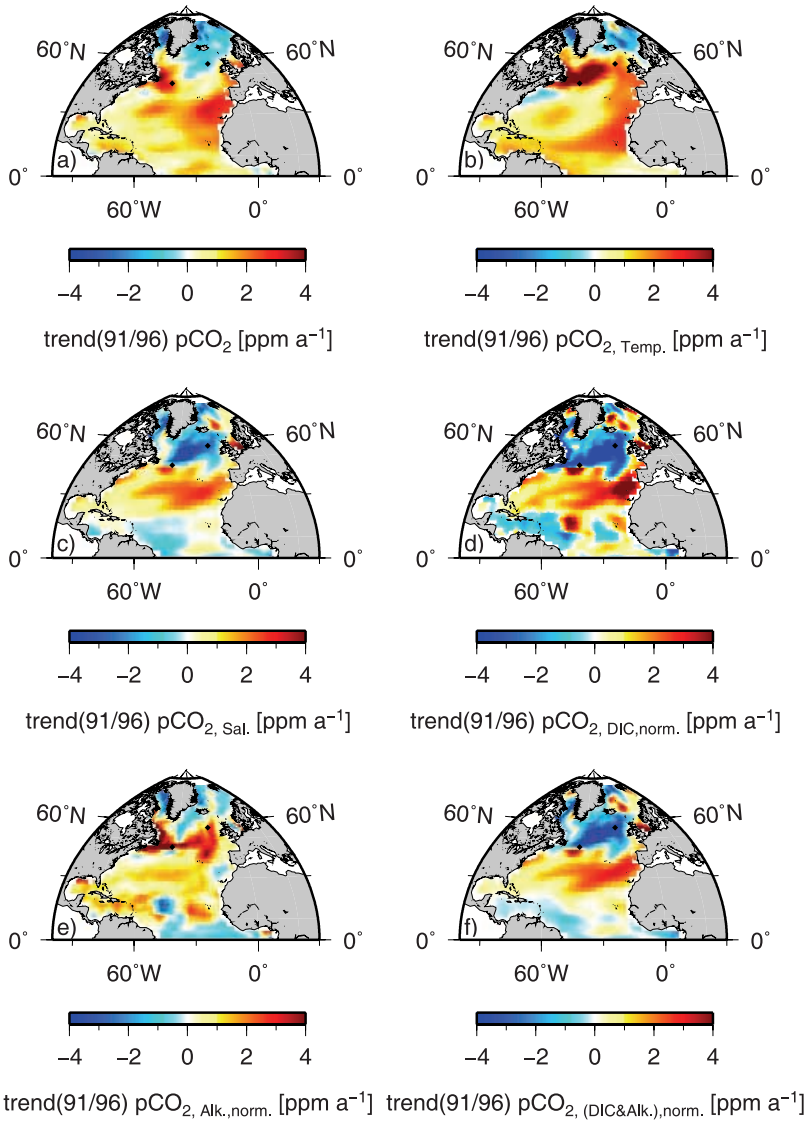

Figure 6. Trend regression analysis of the decomposed pCO_2 changes for preindustrial conditions for the 1991–1996 period according to equation (1). Regressions are shown for (a) the pCO_2 and for the changes in the pCO_2 driven by (b) temperature ($pCO_{2,\ Temp}$), (c) salinity ($pCO_{2,\ Sal}$), (d) DIC_{norm} ($pCO_{2,\ DICnorm}$), (e) A_{Tnorm} ($pCO_{2,\ Alk,norm}$), and (f) simultaneously by DIC_{norm} and A_{Tnorm} ($pCO_{2,\ DICnorm\&Alk,norm}$). The black diamonds indicate the locations at 56.1°N/18.5°W and 45.8°N/43.6°W (see Figures 8 and 9). Please refer to Figure 7 regarding the choice of regression periods.

negative values. NAO-driven variations in wind-driven surface water transport (section 3.1) modify the relative supply of warm, saline, low-DIC_{norm} subtropical water masses from the NAC and cold, fresh, high-DIC_{norm} polar water masses from the Labrador Current (Figure S3). The anticorrelation of salinity and DIC_{norm} at both subpolar gyre locations is evident from the DIC_{norm} versus salinity plot (Figure 10). Note that the relationship is between NAO and the multiannual trends in surface water properties, not necessarily the absolute magnitude of the anomalies themselves. The NAO response at the western location is relatively immediate, while the response at the eastern location is lagged by approximately 2 years reflecting the transport time of the surface waters across the North Atlantic [see, e.g., *Belkin*, 2004].

3.4. Mechanisms Driving Variability of the North Atlantic CO_2 System

[19] We suggest the following mechanism to explain some of the major CO_2 system variability features in the northern North Atlantic. During the early 1990s, a period of positive NAO, increased northeastward NAC transport (Figure 2) enhanced the supply of subtropical high-salinity/low-DIC_{norm} waters, i.e., an enhanced supply of a CO_2 deficiency, to the eastern subpolar gyre. The sea-air ΔpCO_2

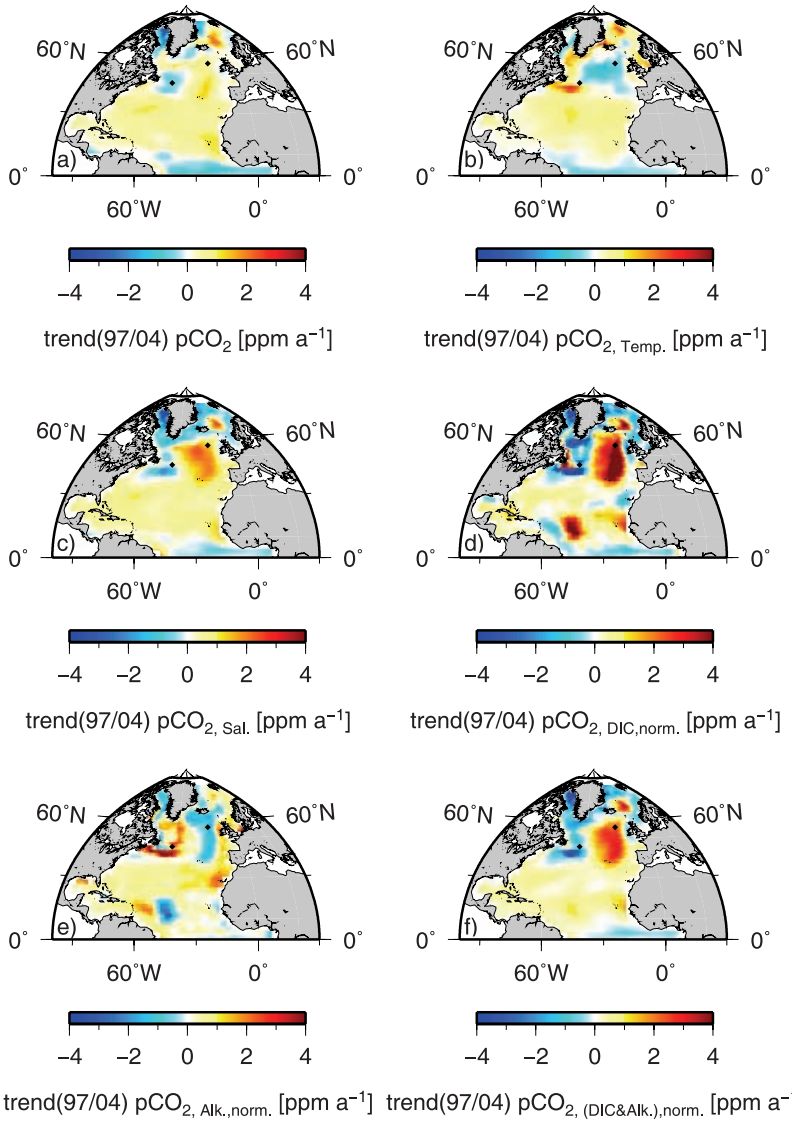

Figure 7. Trend regression analysis of the decomposed pCO_2 changes for preindustrial conditions for the 1997–2004 period according to equation (1). The regression periods have been chosen under consideration of the advective transport time for water masses across the basin, which is approximately 2 years [*Belkin*, 2004]. The regressions thus have been carried out for periods where the biogeochemistry of the entire basin is either under influence of neutral or negative NAO (Figure 7) or positive NAO (Figure 7) conditions. Regressions are shown for (a) the pCO_2 and for the changes in the pCO_2 driven by (b) temperature ($pCO_{2,\ Temp}$), (c) salinity ($pCO_{2,\ Sal}$), (d) DIC_{norm} ($pCO_{2,\ DICnorm}$), (e) A_{Tnorm} ($pCO_{2,\ Alk,norm}$), and (f) simultaneously by DIC_{norm} and A_{Tnorm} ($pCO_{2,\ DICnorm\&Alk,norm}$). The black diamonds indicate the locations at 56.1°N/18.5°W and 45.8°N/43.6°W (see Figures 8 and 9).

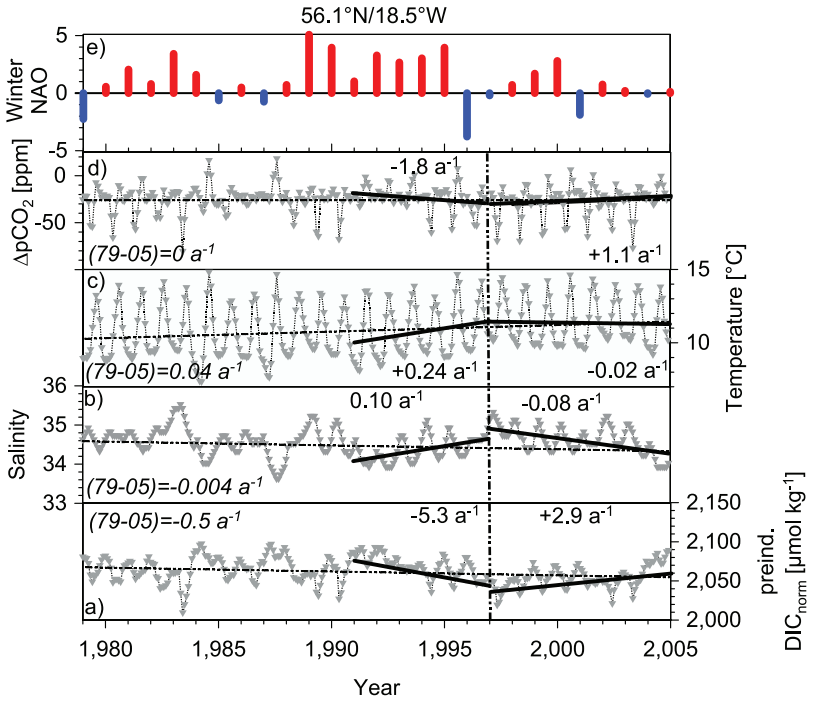

Figure 8. Multiannual variability of preindustrial DIC_{norm}, salinity, temperature, and sea-air ΔpCO_2 at an eastern subpolar gyre location. (a) Preindustrial DIC_{norm}, (b) salinity, (c) temperature, and (d) sea-air ΔpCO_2 at 56.1°N/18.5°W. (e) Wintertime North Atlantic Oscillation (NAO) index. Regressions have been performed for the positive NAO period 1989–1995 and the neutral/negative NAO period 1995–2004. Please note the 2 year lag applied to the eastern station in order to account for advective water mass transport from the western to the eastern basin [*Belkin*, 2004]. The regressions for the entire period 1979 until 2004 are given in italics and by the dotted lines. For comparison with Figures 6 and 7, the slopes of the DIC_{norm} regression lines for the periods 91–96 (-5.4 μmol (kg a)$^{-1}$) and 97–04 (2.9 μmol (kg a)$^{-1}$) as used in Figures 6 and 7 are comparable (not shown).

thus became more negative with time in the eastern subpolar gyre (Figures 6 and 8). The gradual buildup in surface salinity and DIC_{norm} anomalies in the eastern basin due to changes in NAC flow lagged by a couple of years relative to the NAO [see, e.g., *Belkin*, 2004]. The effect of the enhanced intrusion of the Labrador Current Water into the eastern subpolar gyre was minimal relative to the enhanced delivery of subtropical North Atlantic Current Water, evident by the increasing salinity at the eastern subpolar gyre station (Figure 8).

[20] During the early 1990s positive NAO period, the corresponding decreased transport of Gulf Stream/NAC waters to the eastern subtropical gyre resulted in a reduced supply of low-DIC_{norm} water from the west. This lead to positive trends in DIC_{norm} and ΔpCO_2 during positive NAO periods and to opposite trends after 1996 during the subsequent neutral/low-NAO period. The eastern subtropical gyre was thus out of phase with the eastern subpolar gyre in the simulations over the recent observation period.

[21] In the western North Atlantic, positive NAO conditions in the early 1990s caused a northward shift of the intergyre boundary. This resulted in a zonal band east of Nova Scotia of high salinity, negative DIC_{norm}, and negative ΔpCO_2 anomalies along the subtropical/subpolar boundary. Further north off Newfoundland and the Grand Banks, the acceleration of the southward flowing, low-salinity Labrador Current resulted in declining salinity and increasing DIC_{norm} (Figure 9). The ΔpCO_2 trends in this region were somewhat more damped because of a warming trend, which was particularly pronounced in the western subpolar gyre during the 1990s. Some of the warming trends can be attributed to NAO while some may be secular warming due to anthropogenic climate change.

[22] Under neutral or negative NAO conditions from 1996 onward, the above patterns appear to have reversed (Figure 7). For example, the reduced supply of CO_2-deficient water caused positive trends in simulated sea-air ΔpCO_2 and declining CO_2 uptake in the eastern subpolar gyre, similar to observed trends during recent field studies [*Lefèvre et al.*, 2004; *Omar and Olsen*, 2006; *Olsen et al.*, 2006; *Lüger et al.*, 2006; *Corbière et al.*, 2007; *Schuster and Watson*, 2007]. In the model, the surface warming trend in the eastern subtropical gyre (Figure S2) tends to counteract the expected decline in ΔpCO_2 to a certain degree.

[23] Perturbations to these multiannual, NAO-related carbon cycle patterns arise from transient events such as the propagation of surface Great Salinity Anomalies (GSA) around the subpolar gyre. Positive NAO conditions have been related to the occurrence of GSAs, which have been observed as episodic events in the polar and subpolar North

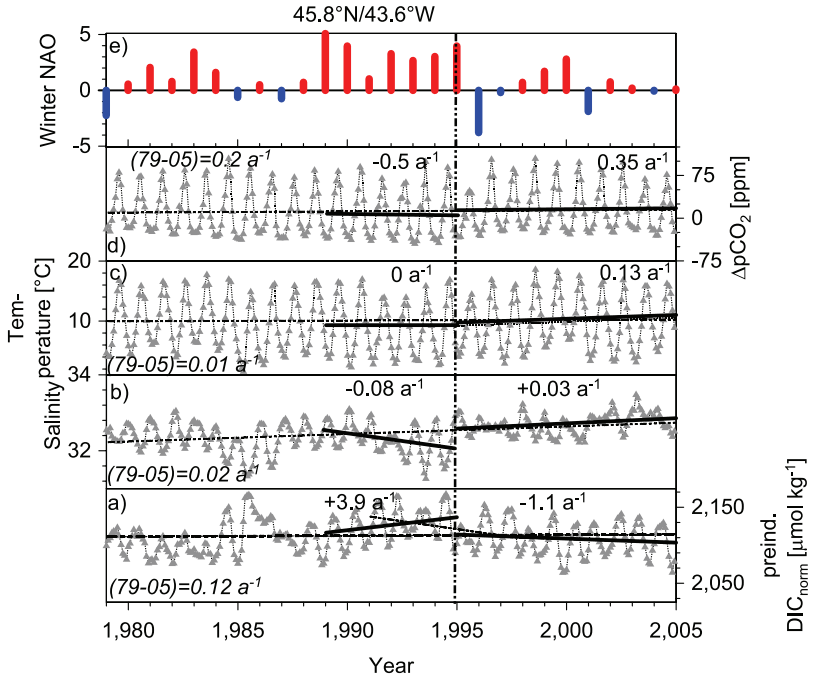

Figure 9. Multiannual variability of preindustrial DIC_{norm}, salinity, temperature, and sea-air ΔpCO_2 at a western subpolar gyre location. (a) Preindustrial DIC_{norm}, (b) salinity, (c) temperature, and (d) sea-air ΔpCO_2 at 45.8°N/43.6°W. (e) Wintertime North Atlantic Oscillation (NAO) index. Regressions have been performed for the positive NAO period 1989–1995 and the neutral or negative NAO period 1995–2004. The regressions for the entire period 1979 until 2004 are given in italics and by the dotted lines. For comparison with Figures 6 and 7, the slopes of the DIC_{norm} regression line for the period 91–96 (shown) are -4.2 μmol (kg a)$^{-1}$ and -0.98 μmol (kg a)$^{-1}$ for the 97–04 period (not shown), respectively.

Atlantic [e.g., *Belkin*, 2004]. Pulses of low-salinity/high-DIC_{norm} waters (Figure 3) intrude into the subpolar gyre via the Labrador Sea and Labrador Current, and GSAs spread across the entire North Atlantic basin on relatively short timescales (1–3 years) via the NAC (Figure 3). These anomalies temporarily reduce CO_2 uptake because of their high-DIC_{norm} characteristics (Figure S4). Our simulation clearly reproduces the GSAs during 1982/1983, 1991 and 1993 [*Belkin*, 2004] (Figure 3).

[24] NAO-driven changes in wind speed constitute another factor that could contribute to CO_2 flux variability [*Doney et al.*, 2008a]. Neutral or negative NAO conditions are characterized by a reduction in wind speed over the subpolar gyre, in particular over the northeastern Atlantic Ocean. These wind conditions would thus act synergistically with the fundamental changes in the surface circulation pattern and support reduced CO_2 uptake during neutral or negative NAO conditions.

[25] The simulated air-sea CO_2 fluxes show a weak, but still significant, correlation with the NAO in two regions, the western subpolar gyre and the eastern North Atlantic north of 60°N (Figure 11). The CO_2 flux–NAO correlation in the western subpolar gyre is positive and strongest at zero phase lag and is caused primarily by surface water pCO_2 responses to varying SST. Substantial cooling under positive NAO phases lowers the pCO_2 and permits higher CO_2 uptake (Figures S4 and S5). The CO_2 flux–NAO correlation in the eastern North Atlantic north of 60°N is negative and strongest with an approximately 2–4 year phase lag. This negative correlation can be attributed to warming (Figure S5) and enhanced delivery of more saline (Figure 3) waters into the polar region, as triggered by the enhanced surface circulation during positive NAO stages. In this region the temperature effect apparently dominates, leading to positive ΔpCO_2 anomalies (Figure 5).

3.5. Comparison of Model CO_2 System Trends With Observations

[26] The positive model 1997–2004 sea-air ΔpCO_2 trends in the eastern subpolar gyre and polar seas (Figure 5d) are consistent with the trends evident from North Atlantic observational studies [*Lefèvre et al.*, 2004; *Omar and Olsen*, 2006; *Olsen et al.*, 2006; *Lüger et al.*, 2006; *Corbière et al.*, 2007; *Schuster and Watson*, 2007], which are based primarily on data from 1995 to 2002/4 (Figure 1). For the same time period, the model eastern subtropical gyre also exhibits positive, but weaker ΔpCO_2 trends. In contrast, the ΔpCO_2 trends for an earlier period 1991–1996 (Figure 5c) are characterized by a strong negative trend in the eastern Atlantic north of approximately 50°N, and by a strong positive ΔpCO_2 trend in the eastern subtropical gyre. Over the full simulation (1979–2004), model surface ocean pCO_2 rises gradually throughout the entire basin, with areas both only slightly exceeding or lagging behind the atmospheric rate of approximately 1.6 ppm a^{-1} as illustrated in the sea-air ΔpCO_2 trends (Figure 5a). To the degree then that the

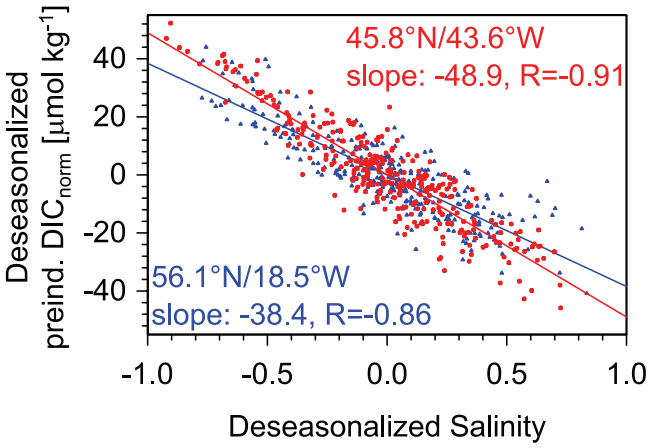

Figure 10. Deseasonalized, preindustrial DIC_{norm} versus deseasonalized salinity for the eastern and western subpolar gyre stations. The red symbols and letters denote the western station at 45.8°N/43.6°W. The blue symbols and letters denote the eastern location at 56.1°N/18.5°W. The contribution from the Labrador Current to the resulting water mass increases in the low-salinity/high-DIC_{norm} direction. The contribution of North Atlantic Current increases in the high-salinity/low-DIC_{norm} direction, respectively. The slopes of the regression lines are given as μmol kg^{-1} (salinity unit)$^{-1}$. See Figure S3 for additional information.

model simulations capture the behavior of the real ocean, we suggest that the observed recent ΔpCO_2 trends may be partially aliasing multiannual variability and do not fully reflect a secular change in the North Atlantic CO_2 sink.

[27] To assess the skill of the model simulations, we compare our model results against field data for four selected regions, with figures provided in the supplement (Figures S6–S8). Observations at Bermuda Atlantic Times Series station (BATS) show the surface water pCO_2 and atmospheric pCO_2 rising at comparable rates [*Bates*, 2001, 2007]. This implies a constant sea-air ΔpCO_2, which is reproduced in our model trends for the full simulation (1979–2004; Figure 5a). The simulations for the BATS region are discussed in detail by *Thomas et al.* [2007]. Further north in the western Atlantic Ocean, *Lüger et al.* [2006] suggest increasing CO_2 uptake, which is in accord with our simulations for some parts of the northwest Atlantic over the 1997–2004 period (Figure 5d). Despite a slight rise of the annual average of the sea surface temperature, the primary cause for this increase appears to be a cooling of the winter surface waters, which lowers the pCO_2 and facilitates CO_2 uptake (Figure S6).

[28] Several studies [*Lefèvre et al.*, 2004; *Omar and Olsen*, 2006; *Olsen et al.*, 2006; *Lüger et al.*, 2006; *Schuster and Watson*, 2007] report declining sea-air ΔpCO_2 and CO_2 uptake in the NAC and eastern subpolar gyre. We show in detail in Figure 12a the simulated and observed pCO_2 time series for one location in the eastern subpolar gyre, where the study areas of *Lüger et al.* [2006] and *Schuster and Watson* [2007] overlap. The observed and simulated surface ocean pCO_2 rise more rapidly than the atmospheric pCO_2, though the observed rise exceeds the simulated one. At this particular location both simulations and observations exhibit an increase in seasonality; however, our simulations reproduce a decrease in the seasonality for regions further northeast as reported by *Schuster and Watson* [2007]. Drivers for these patterns are the increase of winter minimum temperatures as well as a decrease of the summer maximum temperatures. The increase in winter temperature can be attributed to the reduced wintertime cooling of the North Atlantic during neutral or negative NAO phases because of the weakened westerly winds. Furthermore, the NAC slows down during neutral or negative NAO phases leading to a reduced delivery of warmer subtropical water contributing to the cooler summer temperatures (Figure S7). The observed decrease of seasonality [*Schuster and Watson*, 2007] thus might be caused by the decreased seasonality in surface temperature during neutral or negative NAO phases.

[29] Declining sea-air ΔpCO_2 and CO_2 uptake values observed south of Greenland [*Corbière et al.*, 2007] have been assigned to rising temperatures. The simulations for this location (Figures 12b and S8) reproduce the observations, in particular the vanishing of the ΔpCO_2 minima during the 1995–2004 period. For this period, our simulations give a surface water pCO_2 trend of +3.0 ppm a^{-1} while *Corbière et al.* [2007] report +2.5 μatm a^{-1}. Subtracting the rise of atmospheric CO_2 of approx. +1.6 ppm a^{-1} yields a remainder of approximately 1.4 ppm a^{-1} to be explained. Our simulations suggest warming as the major driver for this region (Figure S8), raising surface water pCO_2 by +1.2 ppm a^{-1}. Our simulations further report trends for DIC and A_T of approximately +0.6 μmol DIC (kg a)$^{-1}$ and −0.3 μmol A_T (kg a)$^{-1}$. *Corbière et al.* [2007] did not identify (nor statistically reject) these findings,

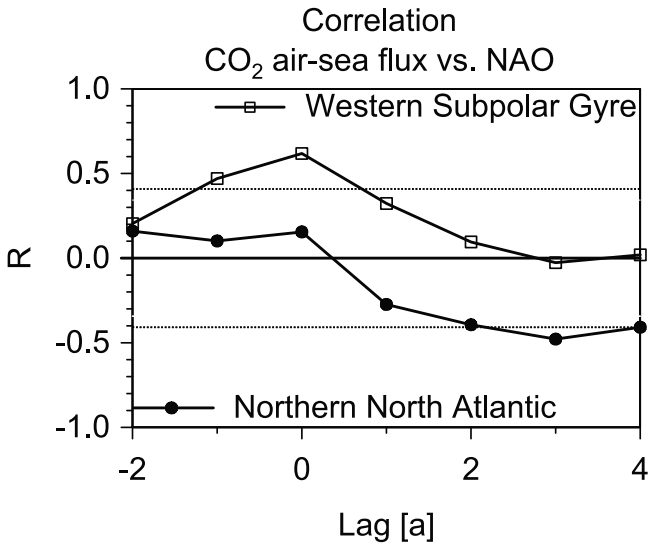

Figure 11. Correlation between CO_2 air-sea fluxes and NAO. CO_2 air-sea fluxes have been correlated versus NAO for two different regions: for the western subpolar gyre between 45°N and 60°N, west of 30°W; and for the northern North Atlantic north of 60°N. The regions above the upper and below the lower dotted lines denote significant correlations with $p < 0.05$.

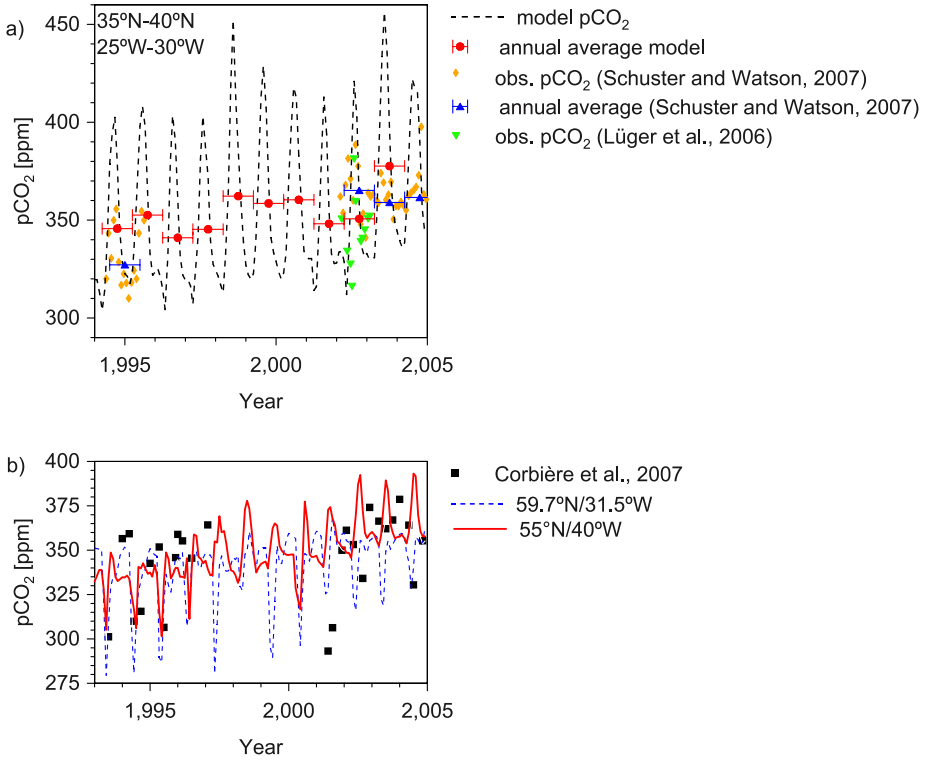

Figure 12. Comparison of field data and simulated data for two locations in the North Atlantic Ocean. (a) Simulations in the northeast Atlantic Ocean in an area where *Lüger et al.* [2006] and *Schuster and Watson* [2007] overlap. The black line represents simulations for this area, and the red symbols give the annual averages, of which time span is indicated by the error bars. Differences to neighboring grid boxes in the area are hardly discernible. Observations by *Lüger et al.* [2006] are given by the green triangles. Orange diamonds give the observations by *Schuster and Watson* [2007]. The corresponding annual averages are indicated by blue triangles, of which time span is indicated by the error bars. Observational and simulated averages have been computed for the same time span. The rise of the surface ocean pCO_2, computed from deseasonalized data is 3.8 ppm a^{-1} for the field data and 2.4 ppm a^{-1} for the simulations. (b) Simulations for the northwest Atlantic Ocean with observations by *Corbière et al.* [2007] and A. Corbière et al. (unpublished data, 2004), which are shown as monthly means for the area between 45°W and 41°W and 53°N and 57°N. The black symbols indicate the field observations, and the simulations are shown for two neighboring grid boxes in the area. Please refer to Figures S6–S8 for more details.

however it has to be noted here that these trends are relatively small and close to the detection limit for observational studies. Perhaps more importantly, the DIC and A_T trends approximately cancel out with respect to pCO_2.

4. Conclusions

[30] Using historical hindcast simulations (1979–2004), we show that the ocean CO_2 system in the temperate North Atlantic exhibits substantial multiannual variability on subbasin scales in response to NAO-driven reorganizations in ocean circulation and surface warming/cooling. The simulated temporal evolution in sea-air ΔpCO_2 is consistent broadly with reported observational trends. We argue that the large CO_2 system trends estimated recently from field data may be heavily influenced by multiannual variability. For example, many of the observational estimates [*Lefèvre et al.*, 2004; *Omar and Olsen*, 2006; *Olsen et al.*, 2006; *Lüger et al.*, 2006; *Corbière et al.*, 2007; *Schuster and Watson*, 2007] cover a period after 1995 of mostly negative or neutral NAO. In our simulations negative or neutral NAO conditions result in reduced NAC transport of warm, saline, low-DIC_{norm} subtropical water into the eastern subpolar gyre, resulting in a substantial decline in CO_2 uptake along the NAC and in the eastern subpolar gyre. We suggest therefore that air-sea CO_2 uptake may rebound in the eastern temperate North Atlantic during future periods of more positive NAO, similar to the patterns found in our model for the sustained positive NAO period in the early 1990s. Our analysis provides support that long-term, coherent ocean carbon observing systems are of critical relevance for the understanding and interpretation of secular changes, associated with climate change and uptake of anthropogenic CO_2 [e.g., *Doney et al.*, 1998b; *Fung et al.*, 2005; *IPCC*, 2001; *Curry et al.*, 2003; *Curry and Mauritzen*, 2005] on the one hand and interannual to interdecadal variability on the other [*Levine et al.*, 2008].

[31] **Acknowledgments.** S. C. Doney and I. D. Lima were supported by NASA grant NNG05GG30G. H. Thomas holds a Canada Research

Chair. We are grateful to an anonymous referee and associate editor C. LeQueré, whose constructive comments greatly helped improve the manuscript. We are grateful to N. Metzl (LOCEAN/IPSL, Paris, France) and H. Lüger for making observational data available. This work contributes to CARBOOCEAN, an EU-FP6 project.

References

Bates, N. R. (2001), Interannual variability of the oceanic CO_2 and biogeochemical properties in the western Atlantic subtropical gyre, *Deep Sea Res., Part II*, *48*, 1507–1528, doi:10.1016/S0967-0645(00)00151-X.

Bates, N. R. (2007), Interannual variability of the oceanic CO_2 sink in the subtropical gyre of the North Atlantic Ocean over the last 2 decades, *J. Geophys. Res.*, *112*, C09013, doi:10.1029/2006JC003759.

Belkin, I. M. (2004), Propagation of the "Great Salinity Anomaly" of the 1990s around the Northern Atlantic, *Geophys. Res. Lett.*, *31*, L08306, doi:10.1029/2003GL019334.

Corbière, A., N. Metzl, G. Reverdin, C. Brunet, and T. Takahashi (2007), Interannual and decadal variability of the oceanic carbon sink in the North Atlantic subpolar gyre, *Tellus, Ser. B*, *59*(2), 168–179, doi:10.1111/j.1600-0889.2006.00232.x.

Curry, R., and C. Mauritzen (2005), Dilution of the northern North Atlantic Ocean in recent decades, *Science*, *308*, 1772–1774, doi:10.1126/science.1109477.

Curry, R., B. Dickson, and I. Yashayaev (2003), A change in the freshwater balance of the Atlantic Ocean over the past four decades, *Nature*, *426*, 826–829, doi:10.1038/nature02206.

Doney, S. C., W. G. Large, and F. O. Bryan (1998a), Surface ocean fluxes and water-mass transformation rates in the coupled NCSR Climate system Model, *J. Clim.*, *11*, 1420–1441, doi:10.1175/1520-0442(1998)011<1420:SOFAWM>2.0.CO;2.

Doney, S. C., J. L. Bullister, and R. Wanninkof (1998b), Climatic variability in upper ocean ventilation rates diagnosed using chlorofluorocarbons, *Geophys. Res. Lett.*, *25*, 1399–1402, doi:10.1029/98GL00844.

Doney, S. C., K. Lindsay, I. Fung, and J. John (2006), Natural variability in a stable 1000 year coupled climate-carbon cycle simulation, *J. Clim.*, *19*(13), 3033–3054, doi:10.1175/JCLI3783.1.

Doney, S. C., S. Yeager, G. Danabasoglu, W. G. Large, and J. C. McWilliams (2007), Mechanisms governing interannual variability of upper ocean temperature in a global hindcast simulation, *J. Phys. Oceanogr.*, *37*, 1918–1938, doi:10.1175/JPO3089.1.

Doney, S. C., I. Lima, R. A. Feely, D. M. Glover, K. Lindsay, N. Mahowald, J. K. Moore, and R. Wanninkhof (2008a), Mechanisms governing interannual variability in the upper ocean inorganic carbon system and air-sea CO_2 fluxes: Physical climate and atmospheric dust, *Deep Sea Res., Part II*, in press.

Doney, S. C., I. Lima, J. K. Moore, K. Lindsay, M. Behrenfeld, T. K. Westberry, N. Mahowald, D. M. Glover, and T. Takahashi (2008b), Skill metrics for confronting global upper ocean ecosystem-biogeochemistry models against field and remote sensing data, *J. Mar. Syst.*, doi:10.1016/j.jmarsys.2008.05.015, in press.

Eden, C., and R. J. Greatbatch (2003), A damped decadal oscillation in the North Atlantic climate system, *J. Clim.*, *16*, 4043–4060, doi:10.1175/1520-0442(2003)016<4043:ADDOIT>2.0.CO;2.

Eden, C., and T. Jung (2001), North Atlantic interdecadal variability: Oceanic response to the North Atlantic Oscillation (1865–1997), *J. Clim.*, *14*, 676–691, doi:10.1175/1520-0442(2001)014<0676:NAIVOR>2.0.CO;2.

Eden, C., and J. Willebrand (2001), Mechanism of interannual to decadal variability of the North Atlantic circulation, *J. Clim.*, *14*, 2266–2280, doi:10.1175/1520-0442(2001)014<2266:MOITDV>2.0.CO;2.

Flatau, M. K., L. Talley, and P. P. Niiler (2003), The North Atlantic Oscillation, surface current velocities, and SST changes in the subpolar North Atlantic, *J. Clim.*, *16*, 2355–2369, doi:10.1175/2787.1.

Friis, K., A. Körtzinger, and D. W. R. Wallace (2003), The salinity normalization of marine inorganic carbon chemistry data, *Geophys. Res. Lett.*, *30*(2), 1085, doi:10.1029/2002GL015898.

Fung, I., S. C. Doney, K. Lindsay, and J. John (2005), Evolution of carbon sinks in a changing climate, *Proc. Natl. Acad. Sci. U. S. A.*, *102*, 11,201–11,206, doi:10.1073/pnas.0504949102.

Greatbatch, R. J. (2000), The North Atlantic Oscillation, *Stochastic Environ. Res. Risk Assess.*, *14*, 213–242, doi:10.1007/s004770000047.

Hurrell, J. W. (1995), Decadal trends in the North Atlantic Oscillation: Regional temperatures and precipitation, *Science*, *269*, 676–679, doi:10.1126/science.269.5224.676.

IPCC (2001), *Climate Change 2001: The Scientific Basis. Contribution of Working Group I to the Third Assessment Report of the Intergovernmental Panel on Climate Change*, edited by J. T. Houghton et al., 944 pp., Cambridge Univ. Press, New York.

Lefèvre, N., A. J. Watson, A. Olsen, A. F. Rios, F. F. Pérez, and T. Johannessen (2004), A decrease in the sink for atmospheric CO_2 in the North Atlantic, *Geophys. Res. Lett.*, *31*, L07306, doi:10.1029/2003GL018957.

Levine, N. M., S. C. Doney, R. Wanninkhof, K. Lindsay, and I. Fung (2008), Ocean carbon system variability and the detection of anthropogenic CO_2, *J. Geophys. Res.*, *113*, C03019, doi:10.1029/2007JC004153.

Lovenduski, N. S., N. Gruber, S. C. Doney, and I. D. Lima (2007), Enhanced CO_2 outgassing in the Southern Ocean from a positive phase of the Southern Annular Mode, *Global Biogeochem. Cycles*, *21*, GB2026, doi:10.1029/2006GB002900.

Lüger, H., R. Wanninkhof, D. W. R. Wallace, and A. Körtzinger (2006), CO_2 fluxes in the subtropical and subarctic North Atlantic based on measurements from a volunteer observing ship, *J. Geophys. Res.*, *111*, C06024, doi:10.1029/2005JC003101.

Moore, J. K., S. C. Doney, and K. Lindsay (2004), Upper ocean ecosystem dynamics and iron cycling in a global three-dimensional model, *Global Biogeochem. Cycles*, *18*, GB4028, doi:10.1029/2004GB002220.

Najjar, R. G., et al. (2007), Impact of circulation on export production, dissolved organic matter and dissolved oxygen in the ocean: Results from Phase II of the Ocean Carbon-cycle Model Intercomparison Project (OCMIP-2), *Global Biogeochem. Cycles*, *21*, GB3007, doi:10.1029/2006GB002857.

Olsen, A., et al. (2006), Magnitude and origin of the anthropogenic CO_2 increase and 13C Suess effect in the Nordic seas since 1981, *Global Biogeochem. Cycles*, *20*, GB3027, doi:10.1029/2005GB002669.

Omar, A. M., and A. Olsen (2006), Reconstructing the time history of the air-sea CO_2 disequilibrium and its rate of change in the eastern subpolar North Atlantic, 1972–1989, *Geophys. Res. Lett.*, *33*, L04602, doi:10.1029/2005GL025425.

Sabine, C. L., et al. (2004), The oceanic sink for anthropogenic CO_2, *Science*, *305*, 367–371, doi:10.1126/science.1097403.

Schuster, U., and A. J. Watson (2007), A variable and decreasing sink for atmospheric CO_2 in the North Atlantic, *J. Geophys. Res.*, *112*, C11006, doi:10.1029/2006JC003941.

Takahashi, T., R. A. Feely, R. F. Weiss, R. H. Wanninkhof, D. W. Chipman, S. C. Sutherland, and T. T. Takahashi (1997), Global air-sea flux of CO_2: An estimate based on measurements of sea-air pCO_2 difference, *Proc. Natl. Acad. Sci. U. S. A.*, *94*, 8292–8299, doi:10.1073/pnas.94.16.8292.

Thomas, H., et al. (2007), Rapid decline of the CO_2 buffering capacity in the North Sea and implications for the North Atlantic Ocean, *Global Biogeochem. Cycles*, *21*, GB4001, doi:10.1029/2006GB002825.

Yeager, S. G., C. A. Shields, W. G. Large, and J. J. Hack (2006), The low resolution $CCSM_3$, *J. Clim.*, *19*(11), 2545–2566, doi:10.1175/JCLI3744.1.

A. Corbière, LOCEAN-IPSL, Université Pierre et Marie Curie, 4, place Jussieu, F-75252 Paris CEDEX, France. (antoine.corbiere@aol.com)

S. C. Doney and I. D. Lima, Department of Marine Chemistry and Geochemistry, Woods Hole Oceanographic Institution, MS 25, 360 Woods Hole Road, Woods Hole, MA 02543-1543, USA. (sdoney@whoi.edu; ilima@whoi.edu)

A. E. Friederike Prowe, Marine Biogeochemistry Research Division, Leibniz-Institut für Meereswissenschaften, IFM-GEOMAR, Düsternbrooker Weg 20, D-24105 Kiel, Germany. (fprowe@ifm-geomar.de)

R. J. Greatbatch, Theoretical Oceanography Department, Leibniz-Institut für Meereswissenschaften, IFM-GEOMAR, Düsternbrooker Weg 20, D-24105 Kiel, Germany. (greatbatch@ifm-geomar.de)

U. Schuster, School of Environmental Sciences, University of East Anglia, Norwich NR4 7TJ, UK. (uschuster@uea.ac.uk)

H. Thomas, Department of Oceanography, Dalhousie University, 1355 Oxford Street, Halifax, NS B3H 4J1, Canada. (helmuth.thomas@dal.ca)

R. Wanninkhof, Ocean Chemistry Division, Atlantic Oceanographic and Meteorological Laboratory, NOAA, 4301 Rickenbacker Causeway, Miami, FL 33149, USA. (rik.wanninkhof@noaa.gov)